Accepted Manuscript

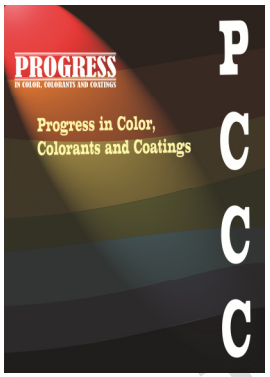

Title: Enhanced Removal of Cochineal Dye from Textile Effluents Using MIL-53 (Al): Optimization, Kinetics, and Thermodynamic Studies

Authors: S. Goudarzi, K. Gharanjig, H. Kazemian, E. Ghasemi, H. Imani, H. Gharanjig, M. Hosseinnezhad, S.M. Etezad

Manuscript number: **PCCC-2403-1289**

To appear in: Progresss in Color, Colorants and Coatings

Received: 11 March 2024

Final Revised: 23 April 2024

Accepted: 24 April 2024

Please cite this article as:

S. Goudarzi, K. Gharanjig, H. Kazemian, E. Ghasemi, H. Imani, H. Gharanjig, M. Hosseinnezhad, S.M. Etezad, Enhanced Removal of Cochineal Dye from Textile Effluents Using MIL-53 (Al): Optimization, Kinetics, and Thermodynamic Studies, Prog. Color, Colorants, Coat., 18 (2025) XX-XXX.

Enhanced Removal of Cochineal Dye from Textile Effluents Using MIL-53 (Al): Optimization, Kinetics, and Thermodynamic Studies

S. Goudarzi[1], K. Gharanjig[1], H. Kazemian[2,3,4], E. Ghasemi[5], H. Imani[1], H. Gharanjig[1], M. Hosseinnezhad[1], S.M. Etezad[6]

[1] Department of Organic Colorants, Institute for Color Science and Technology, P. O. Box: 16765-654, Tehran, Iran.

[2] Materials Technology & Environmental Research (MATTER) lab, P. O. Box: V2N 4Z9, University of Northern British Columbia, Prince George, BC, Canada

[3] Northern Analytical Lab Services (Northern BC's Environment and Climate Solutions Innovation Hub), P. O. Box: V2N 4Z9, University of Northern British Columbia, Prince George, BC, Canada

[4] Environmental Sciences Program, Faculty of Environment, P. O. Box: V2N 4Z9, University of Northern British Columbia, Prince George, British Columbia, V2N4Z9, Canada

[5] Department of Inorganic Glaze and Pigments, Institute for Color Science and Technology, P. O. Box: 16765-654, Tehran, Iran

[6] Department of Environmental Research, Institute for Color Science and Technology, P. O. Box: 16765-654, Tehran, Iran.

Abstract

The treatment of textile dyeing wastewater represents a remarkable environmental challenge, particularly with the use of natural dyes. Despite their more eco-friendly

profile compared to synthetic counterparts, natural dyes contribute to pollution when not fully removed from effluents. Among various remediation techniques, adsorption stands out for its effectiveness, with metal-organic frameworks (MOFs) emerging as promising adsorbents due to their high adsorption capacities and structural stability. This study focuses on the application of a synthesized and characterized MIL-53 (Al) MOF for the adsorption of cochineal extract, a widely used natural red dye in the textile industry, especially handmade carpets. Employing Response Surface Methodology (RSM), we optimized dye removal under varying conditions such as adsorbent amount, temperature, contact time, and pH. Our findings revealed that adsorbent quantity notably influenced the adsorption efficiency, whereas temperature had the least impact, with the highest adsorption capacity observed at 60°C being 178.57 mg/g. Kinetic analyses indicated that the adsorption process conformed to the pseudo-second-order model, suggesting a physical adsorption mechanism, as further evidenced by an activation energy of 4.914 KJ/mol. Thermodynamic parameters, including changes in enthalpy ($\Delta H°$), entropy ($\Delta S°$), and Gibbs free energy ($\Delta G°$), were determined, revealing an endothermic reaction consistent with physical adsorption. The positive enthalpy change and the spontaneous nature of the process, inferred from a negative Gibbs free energy, underscore the potential of MIL-53 (Al) in efficiently removing cochineal dye from wastewater, contributing to the development of sustainable wastewater treatment strategies in the textile industry.

Keywords: Adsorption treatment, Cochineal dye, Dyeing wastewater, MIL-53 (Al), Natural colorants.

1. Introduction

The textile industry considerably contributes to wastewater production, primarily due to its extensive use of water in wet processing, especially in dyeing operations. It is reputed to be the most water-intensive of all industries, with its environmental footprint being a major concern. The discharged wastewater is typically laden with pollutants, posing various environmental impacts. For instance, the presence of colloidal particles and colorants in the water reduces clarity, emits unpleasant odors, and alters its visual appeal. These contaminants can block sunlight penetration, vital for photosynthesis, and disrupt oxygen transfer at the water-air interface. A critical impact of textile wastewater is its reduction of dissolved oxygen levels in aquatic media, essential for aquatic life and the natural waterpurification process. Additionally, effluents seeping into agricultural lands can clog soil pores resulting in diminished soil fertility [1, 2].

Textile dyes fall into two categories based on their nature: synthetic and natural. Synthetic dyes, derived from non-renewable resources, are prevalent in various commercial products. However, they raise environmental and health concerns, including hazardous emissions from manufacturing processes and potential adverse effects on workers and consumers. Certain dyes may pose risks such as respiratory or skin sensitivities [4, 5]. In contrast, natural dyes, known for their lower toxicity, offer functional benefits to fabrics like antibacterial properties, antifungal attributes, UV protection, and insect repellency. However, natural dyeing processes tend to use more colorants than synthetic methods, possibly increasing the pollutant load in wastewater treatment [4, 5]. Consequently, the management of dye house effluents has attracted numerous research attention [6-9].

Cochineal dye, a popular natural colorant, frequently contaminates dye house wastewater, necessitating effective removal strategies. Derived from Dactylopius coccus COSTA and Kermes ilicis aphids, cochineal and its carminic acid derivatives have been used since ancient times for their vibrant red hues in food, cosmetics, paints, beverages, pharmaceuticals, and textile dyeing. The color primarily comes from carminic acid, complemented by smaller amounts of kermesic and flavokermesic acids, and can produce various red shades in textiles by altering mordants and pH levels [10-13].

Effluent treatment strategies include biological, chemical, and physical methods [14-16]. Among these, adsorption stands out for its versatility, cost-effectiveness, simplicity, non-destructive nature, and efficiency. Ideal adsorbents should have high porosity and surface area for effective adsorption. MOFs, with their distinctive properties like high adsorption capacity, thermal stability, longevity, varied compositions, and tunable pore sizes, emerge as superior adsorbents in this context [17, 18]. Incorporating metals like aluminum, iron, vanadium, and zirconium into MOFs is preferred over zinc and copper due to their higher valency, contributing to greater stability. Notably, aluminum's abundance, cost-effectiveness, and lightweight nature make it particularly attractive for MOF production and application [19].

In a review article, the critical need for advanced techniques to eliminate persistent organic pollutants (POPs) like dyes from water due to their harmful effects and resistance to traditional treatment methods is discussed. Highlighting adsorption and photocatalytic degradation as promising solutions, the review underscores the potential of MOFs in addressing POP removal through their customizable structures and high efficiency, providing a significant contribution to water remediation efforts [20].

The MIL (Materials of Institute Lavoisier) type of MOFs has been extensively explored due to their framework flexibility and porous structure with entirely open one-dimensional channels. The MIL series structure helps the adsorption of bulky organic compounds. The benzene rings of MIL-53 aid in π–π stacking between the linker and adsorbate. In a recent work, MIL-53 (Al) was synthesized using a simple solvothermal technique and used to remove Rhodamine B (RhB) from colored wastewater. The Langmuir isotherm and pseudo-second-order kinetic models provide a better fit for dye removal, with a maximum adsorption capacity of 1547 mg/g, primarily through physisorption and endothermic processes [21].

The MIL-53 organometallic skeleton can be modified by altering the center of metal ions or organic ligand derivatives. A hybrid material between metal-organic framework and magnetic material is a promising method for better adsorption. A recent study incorporated magnetic CoFe2O4 nanoparticles and MIL-53 (Al) to create a CFO@MIL-53(Al) nanocomposite for removing Congo red dye. The kinetics and isotherm of adsorption are fitted with Bangham and Temkin models, respectively. Moreover, the maximum absorption capacity using nanocomposite was more than 2 times that of pristine MIL-53 (Al) [22].

In another recent work, an eco-friendly biocomposite combining a metal-organic framework (MIL-53) with Chitosan was developed for pollutant removal. This biocomposite, particularly the surface-functionalized version (SFMOF/BM), exhibited exceptional adsorption capacities for Direct Red 23 dye and pharmaceuticals like tetracycline and doxycycline, reaching up to 12,500 mg/g. The adsorption followed a pseudo-second-order kinetic model, maintaining high efficiency across multiple

regeneration cycles, suggesting its viability as a sustainable solution for removing various organic pollutants from water sources [23].

Researchers synthesized MIL-53 (Fe) and its graphene oxide nanocomposite, enhancing adsorption capabilities, especially for the amine-functionalized MIL-C/GO-NH2(0.3) variant, which demonstrated a remarkable adsorption capacity of 4,504 mg/g for Direct Red 23 dye. The results, following a Langmuir isotherm and pseudo-second-order model, highlight the potential of these materials in efficiently removing similar organic contaminants from water, underscoring their reusability and effectiveness as alternative adsorbents [24].

Many studies have utilized MIL-53 adsorbents for treating colored wastewater due to their advantages including favorable performance, which enables their implementation in industrial settings. To the best of our current knowledge, there is a lack of additional research regarding the utilization of MOFs for the treatment of natural dyes, specially cochineal red dye. Since cochineal is a popular and valuable natural dye in the textile industry, its effluent treatment is of particular importance [10, 25]. This study focuses on developing, characterizing, and employing MIL-53 (Al) for adsorbing cochineal dye from wastewater and explores the adsorption process's various influencing factors and elucidates the removal mechanism through thermodynamic and kinetic analyses.

2. Experimental

2.1. Materials

Terephthalic acid, aluminum nitrate nonahydrate, N,N–dimethylformamide (DMF) were purchased from Merck (Darmstadt, Germany). Ethanol, acetic acid (glacial), sodium

hydroxide (granulated) and hydrochloric acid (36%) were purchased from Dr. Mojallali Industrial Chemical Complex (Tehran, Iran). Cochineal dried insects was prepared from a local dyeing workshop. All the materials used without further purification and aqueous solutions were prepared using deionized water.

2.2. Instrumentation

The BET surface area and pore size determinations were performed using N_2 adsorption-desorption isotherms on a BELSORP MINI II apparatus from Osaka, Japan. For the characterization of the synthesized adsorbents, FE-SEM analysis was conducted using a Zeiss EVO15 microscope in Oberkochen, Germany, XRD measurements were made with a PHILIPS PW1730 spectrometer from Amsterdam, Netherlands, and FT-IR spectra were acquired on a PerkinElmer instrument from Massachusetts, USA. A Sigma sonic SS-15–25 sonifier, operating at 20 kHz and 10 kW, facilitated the sonication step in dye extraction. The absorbance of solutions during adsorption experiments was quantified using a Shimadzu Biospec-1601 spectrometer, based in Kyoto, Japan.

2.3. Synthesis

The MIL-53 (Al) synthesis was conducted using a hydrothermal method, briefly described as follows [26]: A reaction mixture was prepared by dissolving 2.246 g (5.99 mmol) of aluminum nitrate monohydrate and 0.895 g (5.38 mmol) of terephthalic acid in 30 mL of DMF. This mixture was stirred at room temperature for 15 minutes before being transferred to a 45 mL Teflon-lined stainless-steel autoclave. The autoclave contents were then heated to 150°C for 5 hours. Post-reaction, the solid product was

separated via centrifugation at 4500 rpm, washed with DMF and acetone, and dried at 150°C for 17 hours to remove unreacted precursors and residual solvents. Finally, the powder was further purified by heating at 333°C for 3 days.

2.4. Extraction of Dye

The procedure for extracting cochineal dye is outlined as follows [13]: A 60:40 mixture of water and ethanol was used to extract the dye from 120 grams of finely ground cochineal in 2000 ml of the solvent mixture. The mixture underwent ultrasonication for 20 minutes at 50°C with a 10 kW, 20,186 Hz ultrasound device. This was followed by stirring the mixture for 1 hour at 60°C to ensure thorough mixing. The resulting solution was then filtered through filter paper to separate the dye extract.

2.5. Adsorption Experiments

The adsorption process was optimized using RSM [27, 28]. The experiments were designed and analyzed using Design Expert software (Version 12.0.3.0, State-Ease, Minneapolis, MN). Initially, a 0.2 g/l cochineal solution was prepared by diluting 10 ml of the dye solution in 30 ml of deionized water. The initial absorbance (A_i) of this solution was measured at the dye's maximum absorption wavelength. Experiments were then conducted to study the dye removal efficiency of MIL-53 (Al) under various conditions of pH, contact time, temperature, and adsorbent concentration, keeping all other factors constant.The absorbance intensity of the solution post-adsorption (A_f) was measured to determine the percentage of dye removal ($R\%$), calculated using equation 1. A total of 30 experiments were performed, including 6 replicates to ensure accuracy and

reproducibility. Table 1 presents the range of experimental conditions explored (Eq. 1). It should be noted that pH values of 3, 6, and 9 are adjusted to 0.1 M hydrochloric acid, 0.1 M acetic acid, and 0.1 M sodium hydroxide, respectively .

$$Dye\ removal\ (\%) = \left(\frac{A_i - A_f}{A_i}\right) \times 100 \quad \textbf{(1)}$$

Table 1. Variables, ranges, and levels used for RSM.

Variables	Rage and levels		
	-1	0	+1
A: T (°C)	30	45	60
B: t (min)	10	65	120
C:pH	3	6	9
D: MOF amount (g)	0.005	0.025	0.045

2.6. Adsorption kinetic

To investigate the adsorption kinetics, a 20 mL aliquot of the 0.2 g/L cochineal dye solution was diluted with 60 mL of deionized water, achieving a 1:3 volume ratio, and adjusted to the optimal pH. The solution was then stirred for 15 minutes to attain the target temperature. Following this, the calculated optimal amount of the MOF adsorbent was introduced into the mixture, marking the commencement of the timing. Sampling occurred at intervals of 5, 10, 15, 20, 30, 40, 50, 60, 80, 100, and 120 minutes post-adsorbent addition. The adsorption intensity of each sample was measured using UV-Vis spectroscopy after the separation of the adsorbents. This experiment was replicated at three distinct temperatures: 30, 45, and 60 °C. The collected data were then analyzed using the linear forms of the pseudo-first-order, pseudo-second-order, and intraparticle

diffusion kinetic models. The model that best described the relationship between the dye removal efficiency and contact time was identified based on the goodness of fit.

2.7. Adsorption Isotherms

To establish the adsorption isotherms, six solutions of varying concentrations were prepared by mixing different ratios of deionized water and the 0.2 g/L cochineal dye solution, as detailed in Table 2. Each solution was then equilibrated at the desired temperature for 15 minutes. Subsequently, 0.025 g of the MOF adsorbent was added to each solution, which was then stirred continuously for 3 hours. After this period, samples were extracted from each solution for analysis. The adsorbent particles were separated from the samples, and the adsorption capacities were quantified using UV-Vis spectroscopy to assess the efficiency of dye removal across the different dye concentrations.

Table 2. Concentration of dyes used for thermodynamic studies.

Variations	1	2	3	4	5
Amount of dye (mL)	10	20	30	40	50
Total volume of solution (mL)	80	80	80	80	80
Dye concentration (mg/L)	25	50	75	100	125

3. Results and Discussion

3.1. Characterization of MOF

The FT-IR spectroscopy analysis provided essential insights into the molecular structure

of the synthesized MOF, MIL-53 (Al). The spectrum, depicted in Figure 1-a, highlights characteristic peaks within the 1400–1700 cm^{-1} range, which are indicative of carbonyl groups coordinating with aluminum ions. Specifically, the peaks observed at 1604, 1508, and 1417 cm^{-1} are attributed to the C=O groups bonded with aluminum. The presence of an asymmetric C=O stretch is notably marked by the peak at 1508 cm^{-1} [29]. Furthermore, the spectral region between 1604 and 1448 cm^{-1} encompasses the vibrations of aromatic carbon-carbon double bonds, which likely overlap with those of the coordinated entities. The aromatic C-H stretching vibrations are discernible at 3085 cm^{-1}, further confirming the presence of an aromatic framework within the MOF structure [26]. Nitrogen adsorption-desorption isotherm analysis, conducted via the BET method, revealed the specific surface areas of MIL-53 (Al) to be 1451.6 m^2/g and 1438.9 m^2/g based on BET and Langmuir calculations, respectively. According to the International Union of Pure and Applied Chemistry (IUPAC) classification, the observed type II isotherm with an H3 hysteresis loop, as illustrated in Figure 1-b, suggests a microporous structure within MIL-53(Al). This is further evidenced by the detailed analysis presented in Table 3, which underscores the MOF's substantial microporous nature.

Table 3. Adsorption isotherm analysis of MIL-53 (Al).

Specific Volume/ surafe	Langmuir	t-plot	Harkins–Jura	BET	mean pore diameter (nm)
V(cm^3/g)	330.6	0.44	1.15	333.5	4.6
a(m^2/g)	1438.9	3.106	208.9	1451.6	

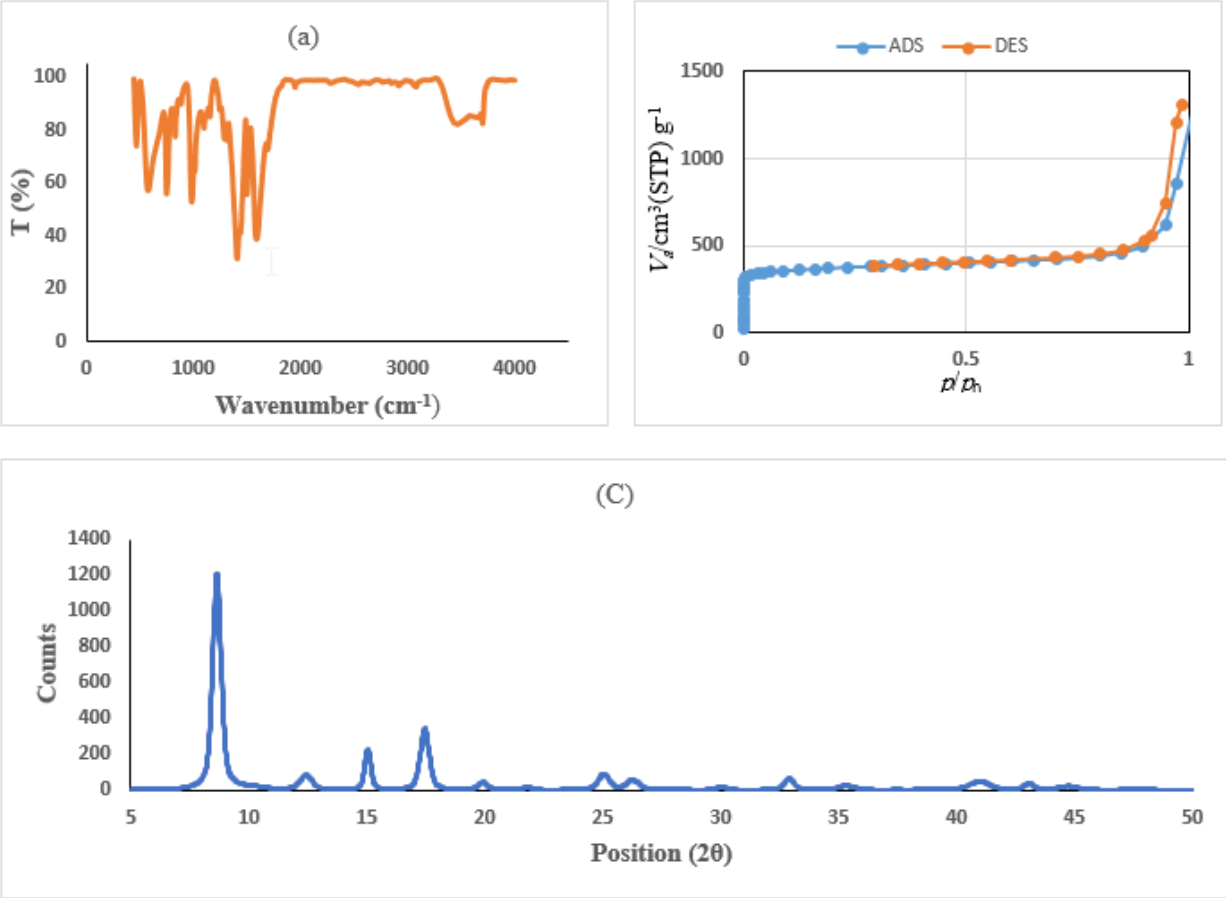

Figure 1. Characterization of synthesized MOF, a: FT-IR, b: BET analysis, and c: XRD.

The XRD pattern of MIL-53 (Al), shown in Figure 1c, provides additional confirmation of the MOF's crystalline structure. The distinct diffraction peak at 2θ 8.65°, corresponding to the (110) reflection, along with a significant peak at 2θ 17.45° that merges the (211) and (220) reflections, aligns with previously reported structures, indicating the successful synthesis of crystalline MIL-53 (Al) [26].

FE-SEM analysis offered visual confirmation of the MOF's morphology. As depicted in Figure 2, the spherical particles of MIL-53 (Al) are uniformly distributed with a size below 50 nm, showcasing the homogeneity and nano-scale size of the synthesized MOF. This morphological feature is expected to contribute positively to the MOF's adsorption capabilities due to the increased surface area and accessibility of active sites.

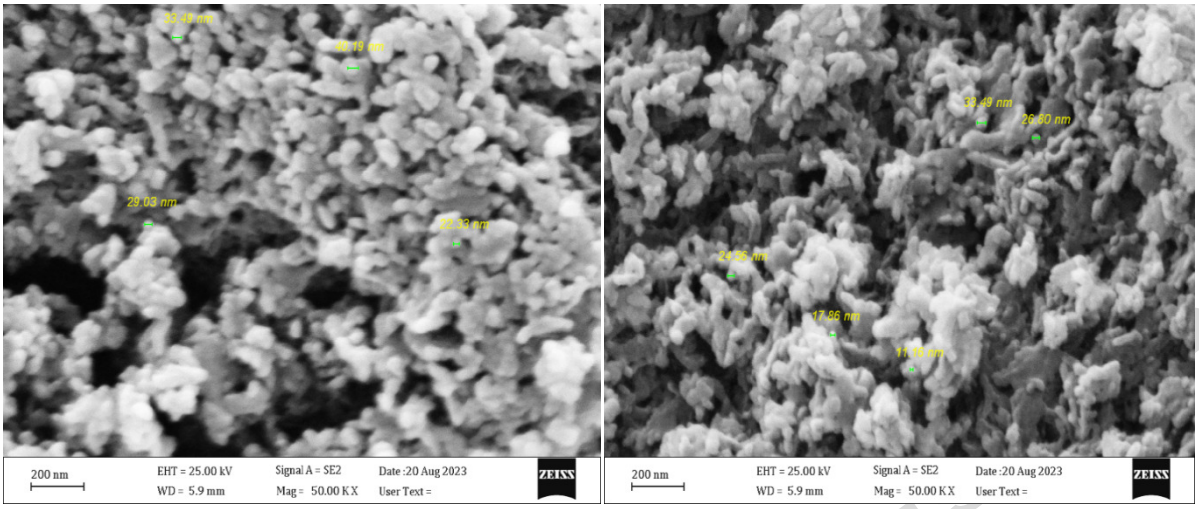

Figure 2. FE-SEM images of MIL-53 (Al).

3.2. Adsorption and optimization

The impact of various parameters on the adsorption process and its optimization was explored using the RSM. The designed experiments, outlined in Table 4, investigated the effects of temperature *(A)*,contact time *(B)*, pH*(C)*, and adsorbent amount *(D)* on dye removal efficiency. Remarkably, Experiment 16 showcased an exceptional dye removal rate of 99.53%, highlighting the efficacy of the chosen conditions. The consistency in results from the duplicate experiments (25 to 30) underscored the process's reproducibility.

Table 4. Results of the designed experiment for the adsorption of dye on MIL-53 (Al) by RSM method.

Number	*A: T*	*B: t*	*C: pH*	*D: MOF*	*R%*
1	30	10	3	0.005	15.83
2	60	10	3	0.005	21.11
3	30	120	3	0.005	32.6

4	60	120	3	0.005	24.84
5	30	10	9	0.005	5.16
6	60	10	9	0.005	13.97
7	30	120	9	0.005	1.39
8	60	120	9	0.005	30.9
9	30	10	3	0.045	89.22
10	60	10	3	0.045	83.85
11	30	120	3	0.045	86.18
12	60	120	3	0.045	76.86
13	30	10	9	0.045	26.08
14	60	10	9	0.045	84.47
15	30	120	9	0.045	88.35
16	60	120	9	0.045	99.53
17	30	65	6	0.025	85.38
18	60	65	6	0.025	81.83
19	45	10	6	0.025	35.71
20	45	120	6	0.025	81.67
21	45	65	3	0.025	79.65
22	45	65	9	0.025	53.1
23	45	65	6	0.005	17.54
24	45	65	6	0.045	91.61
25	45	65	6	0.025	72.51
26	45	65	6	0.025	73.11
27	45	65	6	0.025	73.2
28	45	65	6	0.025	72.1
29	45	65	6	0.025	71.49
30	45	65	6	0.025	71.3

Subsequently, four distinct models including linear, 2-factor interaction (2FI), quadratic, and cubic were assessed to identify the most suitable equation for the adsorption process. The quadratic model emerged as the preferred choice, as indicated in Table 5, due to its superior correlation coefficient and standard deviation. With a correlation coefficient of 0.92, the quadratic model demonstrates a satisfactory level of fit to the adsorption data.

Table 5. Proposed statistical model for optimization of the adsorption process.

Source	*SD*	R^2	*Adjusted* R^2	*Press*
Linear	17.5	0.7184	0.6734	11558.11
2FI	17.97	0.7743	0.6555	23502.77
Quadratic	11.39	0.9285	0.8617	13247.71
Cubic	6.67	0.9886	0.9526	76001.92

Variance analysis, presented in Table 6, identified the adsorbent amount as the most significant factor influencing cochineal dye adsorption. Interestingly, the p-value for temperature was above 0.05, suggesting that temperature variations had a minimal impact on the adsorption outcome. Optimal adsorption conditions were derived from equation 2, with Figure 3 illustrating the marginal effects of each parameter. Temperature showed a negligible effect on dye adsorption, with a slight decrease followed by an increase in adsorption as temperature rose. Contact time marginally enhanced dye adsorption, indicating a less pronounced influence. The pH level significantly affected dye adsorption, with acidic conditions favoring higher adsorption rates compared to alkaline environments. The adsorbent amount emerged as the most critical factor, with increased quantities significantly boosting dye adsorption efficiency (Eq. 2).

Table 6. Effect of different parameters on adsorption calculated by analysis of variance.

Source	Sum of Squares	df	Mean Square	F-value	P-value	
Model	25243.02	14	1803.07	13.91	0.0001<	significant
A-T	491.93	1	491.93	3.8	0.0704	
B-t	1314.99	1	1314.99	10.14	0.0061	
C-pH	558.45	1	558.45	4.31	0.0555	

D-MOF	17166.81	1	17166.81	132.43	0.0001<	
AB	158.95	1	158.95	1.23	28.56	
AC	872.17	1	872.17	6.73	0.023	
AD	42.15	1	42.15	0.33	0.577	
BC	333.88	1	333.88	2.58	0.129	
BD	102.87	1	102.87	0.79	0.039	
CD	9.32	1	9.32	0.072	0.79	
A2	364.86	1	364.86	2.81	0.11	
B2	441.11	1	441.11	3.4	0.08	
C2	74.52	1	74.52	0.57	0.46	
D2	763.21	1	763.21	5.89	0.03	

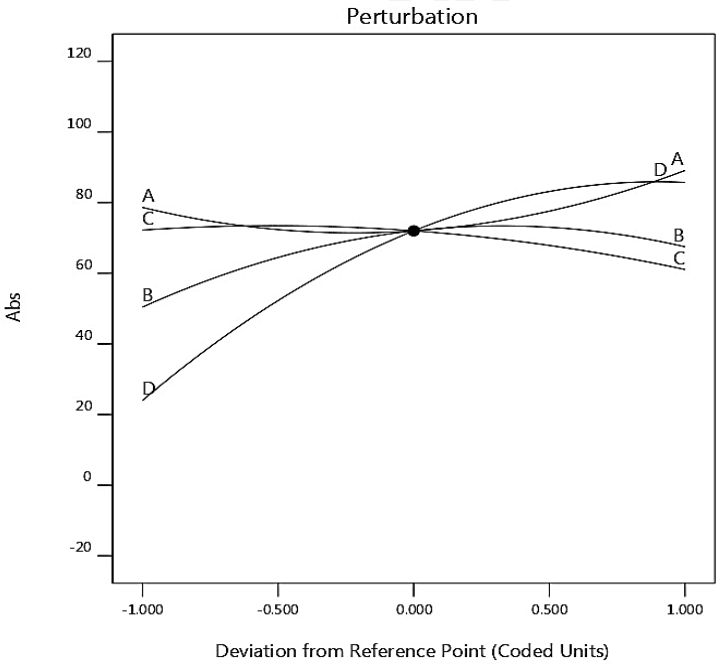

Figure 3. Linear diagram showing the effect of different parameters on the adsorption process.

$$R\% = 114.7 - 5.2A + 0.66B - 4.2C + 3219.8D - 0.003AB + 0.16AC + 5.4AD + 0.02BC + 2.3BD + 12.7CD + 0.05A2 - 0.004B2 - 0.59C2 - 42907.9D2 \quad (2)$$

The interactive effects of the four parameters are depicted in the three-dimensional plots of Figure 4. These diagrams allow for a comparative analysis of the impact of two variables at a time, with the remaining two held constant at their central values. The visual representation in Figure 4 highlights the significant influence of adsorbent quantity on dye adsorption efficiency. It is evident that using the maximum quantity of adsorbent leads to optimal adsorption. Additionally, within the context of the highest adsorbent levels, an increase in adsorption efficiency is observed with rising temperatures and more acidic conditions.

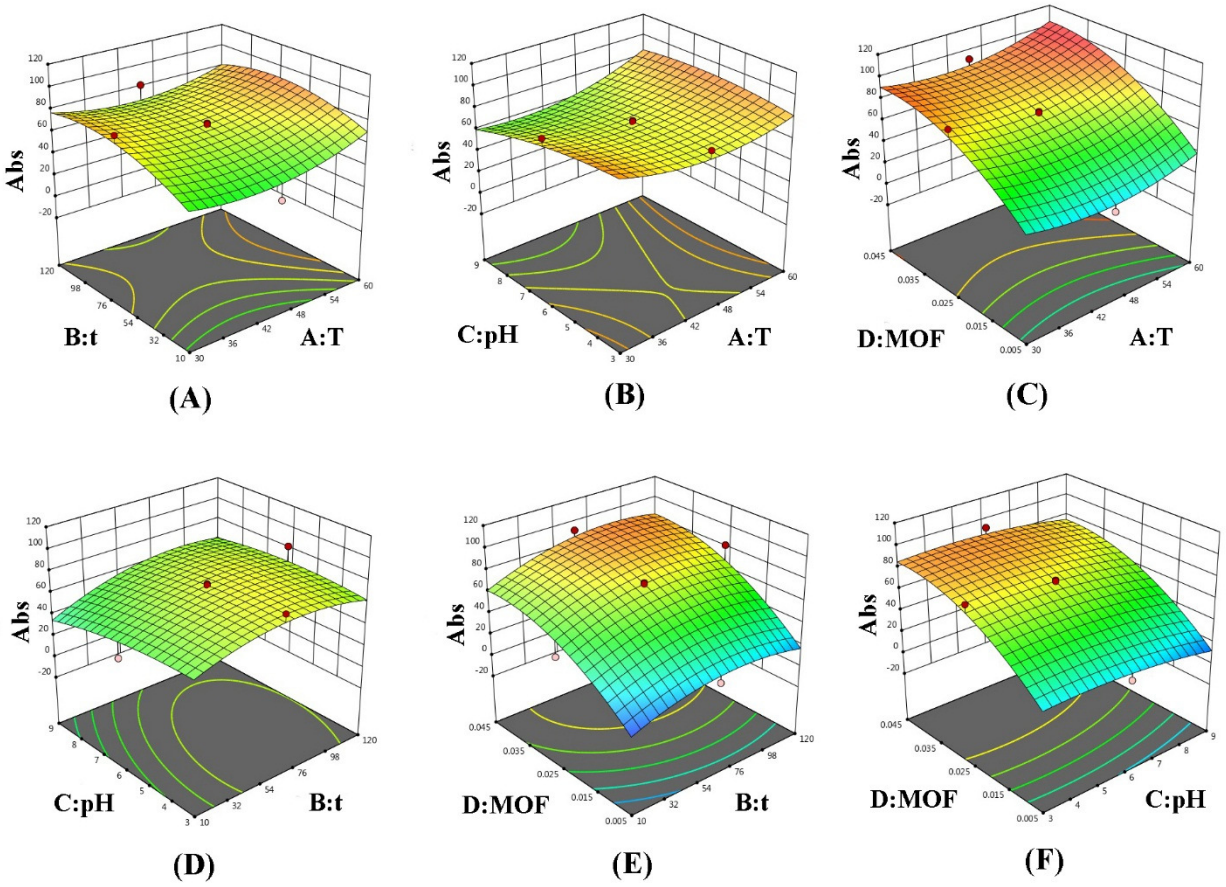

Figure 4. Three-dimensional diagrams of the mutual effects of four factors in the adsorption process.

Table 7 compares the experimentally determined dye removal percentages with those

predicted by the model, revealing an average error percentage below 3% across all samples. This close agreement validates the suitability of the chosen models for describing the adsorption process under optimal conditions, confirming the effectiveness of MIL-53 (Al) in removing cochineal dye from solutions.

Table 7. The optimum conditions of dye adsorption.

No.	A	B	C	D	Theoretical R%	Experimental R%	Error percentage	Desirability
1	45	65	6	0.045	94	91.61	2.5%	1
2	60	120	9	0.045	100	99.53	0.47%	1

3.3. Kinetic studies

The adsorption behavior of MIL-53 (Al) towards cochineal dye was scrutinized at temperatures of 30, 45, and 60 °C. Kinetic parameters such as the initial concentration (C_0), equilibrium concentration (C_e), and concentration at any given time t (C_t) were measured to assess the adsorption dynamics. These concentrations were pivotal in calculating the quantities of dye adsorbed at equilibrium (q_e) and at any given time (q_t), as prescribed by equations 3 and 4, with$V$ and Mdenoting the solution volume and adsorbent mass, respectively. The kinetic analysis was conducted using the linear forms of the pseudo-first order, pseudo-second order, and intraparticle diffusion models, characterized by rate constants k_1, k_2, and k_{ID}, as delineated in equations (5-7) [30, 31].

$$q_e = \frac{V(C_0 - C_e)}{M} \quad (3)$$

$$q_t = \frac{V(C_0 - C_t)}{M} \quad (4)$$

$$log(q_e - q_t) = -\frac{k_1}{2.303}t + log\, q_e \quad (5)$$

$$\frac{1}{q_t} = \frac{1}{k_2 q_e^2}\left(\frac{1}{t}\right) + \frac{1}{q_e} \quad (6)$$

$$q_t = k_{ID}\sqrt{t} + I \quad (7)$$

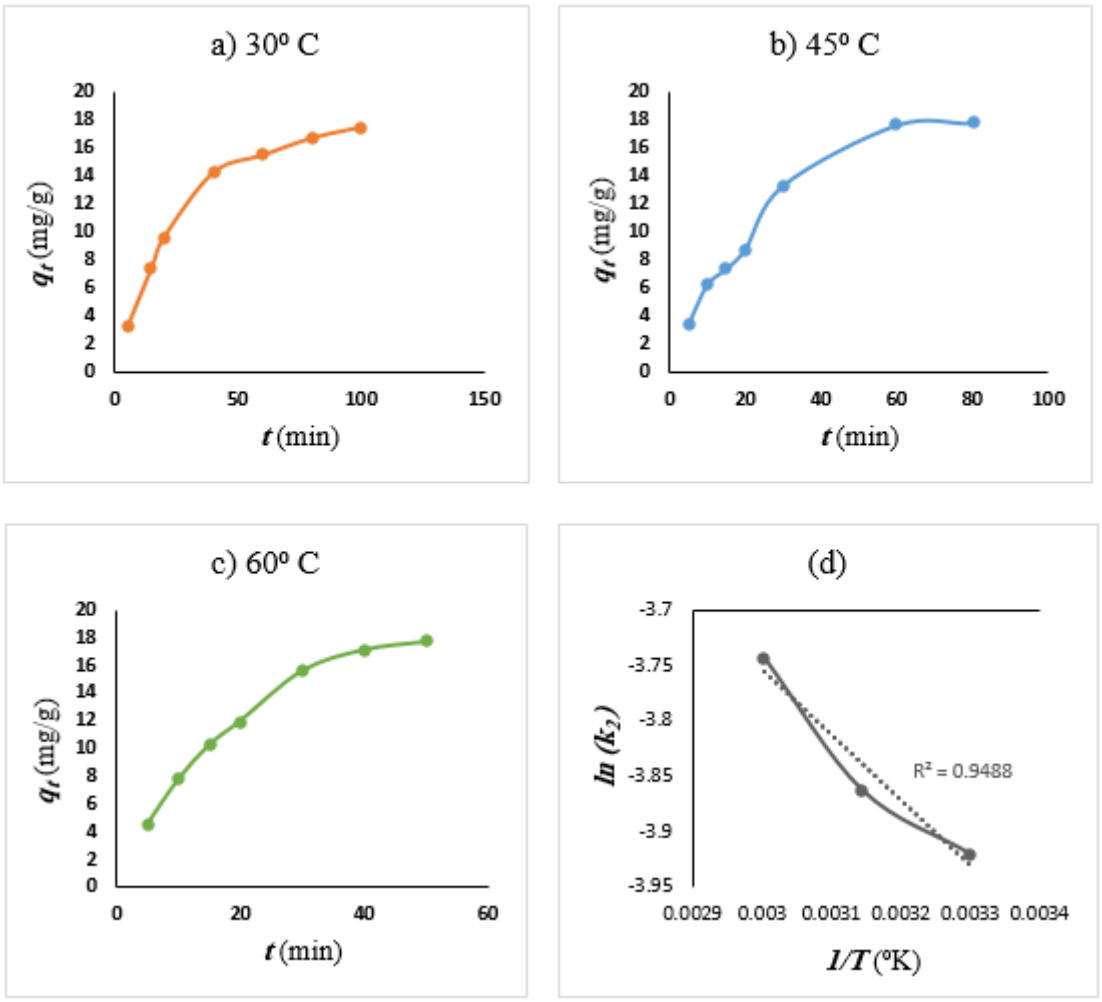

Figure 5. Kinetic experiments in temperatures of a) 30, b) 45, c) 60 0C, and d) Arrhenius linear equation.

Time-dependent changes in q_t, depicted in Figure 5a-c, facilitated the comparison of these kinetic models. The model fitting results, reported in Table 8, were derived from the linear representations of the pseudo-first order, pseudo-second order, and intraparticle

diffusion models. Each model's correlation coefficients were computed across the different temperatures. Among these, the pseudo-second-order model, with a correlation coefficient of 0.99 for all tested temperatures, was identified as the most representative of the adsorption process, indicating an abundance of active sites on the adsorbent [32]. The model's reliance on the squared term (q_e-q) emphasizes the potential for adsorption rate deceleration as the available sites become increasingly occupied, a scenario particularly applicable when the dye molecules exactly match the number of active sites on the adsorbent [33].

Table 8. Fitting results of kinetic experiments.

Model	Linear form	T (°C)	R^2	k_2 (g/mg min)
Intraparticle diffusion	q_t vs. $t^{0.5}$	30	0.94	
		45	0.95	
		60	0.97	
Pseudo-first-order	log (q_e-q_t) vs. t	30	0.85	
		45	0.90	
		60	0.91	
Pseudo-second-order	1/q_t vs. 1/t	30	0.99	1.19×10^{-3}
		45	0.99	1.26×10^{-3}
		60	0.99	1.42×10^{-3}

The adsorption mechanism, inferred from the activation energy, was determined using the Arrhenius equation (equation 8), whereΔEsignifies the activation energy, T is the temperature in Kelvin, and k is the rate constant. This energy was calculated by plotting the logarithm of the rate constant against $1/T$ [34]. The resulting plot in Figure 5-d, based on the best-fit pseudo-second-order model, yielded an activation energy of 4.914 KJ/mol, indicative of physical adsorption for activation energies below 40 KJ/mol [35]. This suggests that the interaction between MIL-53 (Al) and cochineal dye is likely governed by weak π-π stacking interactions, in the absence of strong chemical bonds [36].

$$\ln K = \ln k_0 - \frac{\Delta E}{RT} \quad (8)$$

3.4. Thermodynamics studies

The elucidation of adsorption mechanisms necessitates an analysis of equilibrium data, often represented through adsorption isotherms. These isotherms play a vital role in clarifying the interactions between adsorbate molecules or ions and the adsorbent surface sites. Thus, employing a theoretical or empirical equation to model the equilibrium data is essential for interpreting and predicting adsorption behaviors. An adsorption isotherm is essentially a mathematical model that describes the relationship between the quantity of solute adsorbed onto the adsorbent and the solute concentration in the liquid phase [37]. To ascertain the thermodynamic parameters of the adsorption process, it's pivotal to first determine the appropriate adsorption isotherm model and its constants. After experimental data are fitted to various isotherm models, the most suitable ones are identified, and their constants are used to analyze the thermodynamic constants and the underlying adsorption mechanism. Typically, adsorption isotherms adhere to the Langmuir, Freundlich, and Temkin models, illustrated in equations 9-11, respectively.The Langmuir model, defined by q_{max} (mg/g) as the maximal adsorption capacity and$K_L$as the Langmuir constant related to adsorption energy, suggests monolayer adsorption on a homogeneous surface. In the Freundlich model (Eq. 10), K_F represents the Freundlich constant and *1/n*denotes the heterogeneity factor, reflecting the surface heterogeneity of the adsorbent [36]. The Temkin isotherm, embodied by parameters A and B in equation 11, considers the interactions between adsorbent and adsorbate [37]. Figure 6a-c depicts the adsorption isotherms at varying temperatures of 30, 45, and 60

°C. The results of the isotherm fitting are detailed in Table 9, providing insight into the adsorption process at different temperatures and enabling the derivation of thermodynamic parameters.

$$\frac{C_e}{q_e} = \frac{1}{K_L q_{max}} + \frac{C_e}{q_{max}} \quad (9)$$

$$\ln q_e = \ln K_F + \frac{1}{n} \ln C_e \quad (10)$$

$$q_e = B \ln C_e + B \ln A \quad (11)$$

The adsorption isotherm analysis compared the experimental data with three models, revealing that cochineal dye adsorption onto MIL-53 (Al) aligns with the Langmuir isotherm model. This suggests that optimal adsorption is achieved when the adsorbent surface forms a monolayer of adsorbate molecules, indicating uniform adsorption sites with identical energy levels and no lateral movement of adsorbate molecules across the homogeneoussurface of adsorbent.In other words, once a molecule reaches a specific spot, there is no more adsorption occurring at that spot. The Langmuir model also infers that adsorption forces diminish with increasing distance from the surface [38, 39].

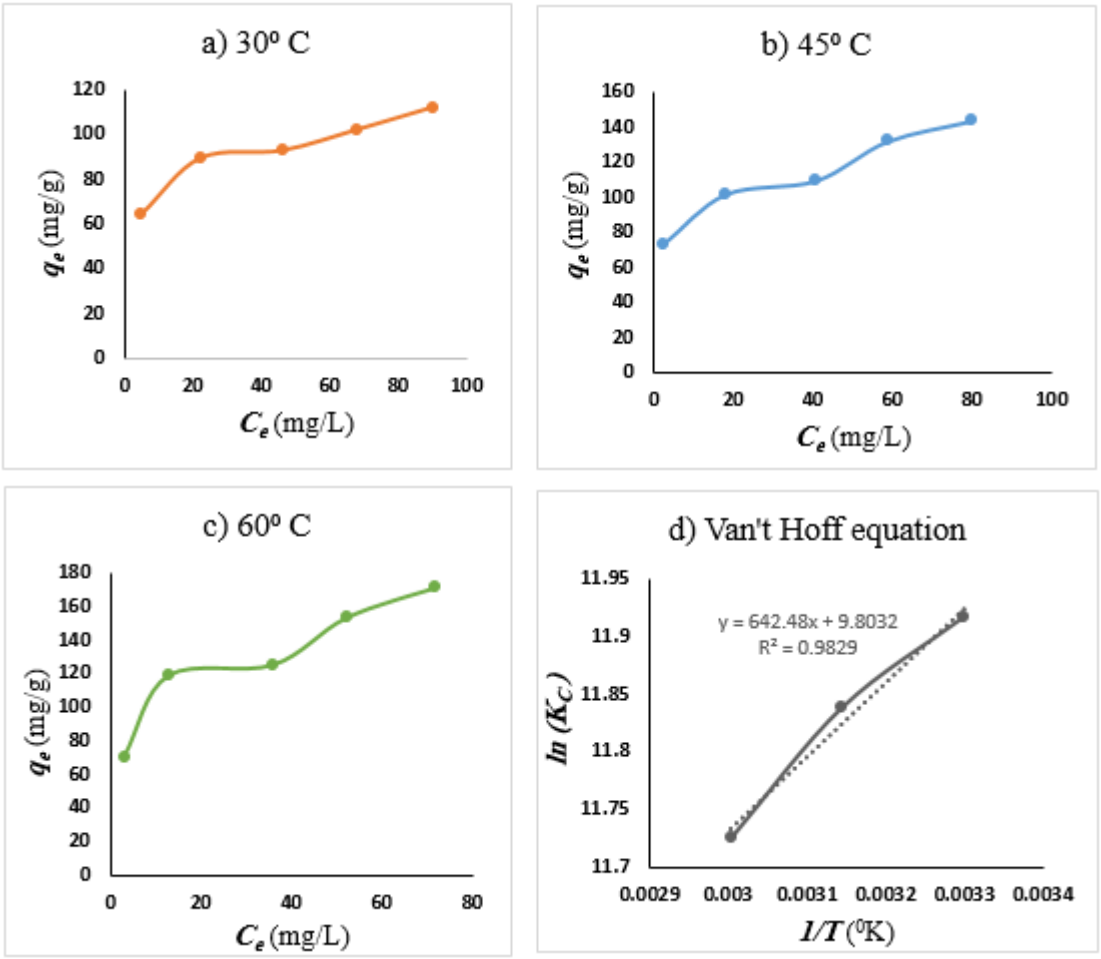

Figure 6. Adsorption isotherms of cochineal dye on MIL-53 (Al) in various temperatures.

Table 9. Fitting results of thermodynamic experiments.

Model	Linear form	T (°C)	R^2	K_L (L/mg)	q_m (mg/g)
Temkin	q_e vs. Ln C_e	30	0.95		
		45	0.90		
		60	0.93		
Freundlich	C_e/q_e vs. C_e	30	0.96		
		45	0.95		
		60	0.94		
Langmuir	Ln q_e vs. Ln C_e	30	0.98	0.149741	114.94
		45	0.97	0.138433	149.25
		60	0.97	0.123621	178.57

Various parameters influence the adsorption capacity of MOFs in the removal of dyes. The significance of MOFs lies in their specific surface area, pore volume, and pore

diameter size. Furthermore, the medium conditions, such as temperature, have a major effect [40]. According to the results shown in Table 10, an increase in temperature is associated with a higher adsorption capacity. The highest recorded value of q_{max} is 178.57 mg/g at a temperature of 60°C. Meanwhile, based on the findings shown in Table 10, an investigation was conducted to determine the maximum adsorption capacity of various dyes with different structures and natures using pristine MIL-53 adsorbents. The results indicate that cochineal natural dye exhibited acceptable adsorption on MIL-53 (Al).

Table 10. Adsorption capacity of different dyes using MIL-53 adsorbents.

Adsorbent	Dye	Nature of dye	Maximum adsorption capacity (mg/g)	Ref
MIL- 53 (Al)	Methyl orange	Synthetic	219.4	[41]
MIL-53 (Al)	Malachite green	Synthetic	143.5	[41]
MIL-53 (Fe)	Methyl red	Synthetic	183.5	[42]
MIL-53 (Fe)	Direct red 23	Synthetic	3100	[21]
MIL-53 (Al)	Rhodamine B	Synthetic	1547	[21]
MIL-53 (Al)	Congo red	Synthetic	15.295	[22]
MIL-53 (Al)	Cochineal	Natural	178.57	Present work

Thermodynamic analysis of adsorption experiments is pivotal to ascertain the spontaneity and viability of the adsorption process. By employing experimental data using equations 12-14, key thermodynamic parameters such as Gibbs free energy change *($\Delta G°$),* enthalpy change *($\Delta H°$),* and entropy change *($\Delta S°$)* are computed. The derivation of *Kc* values from the Langmuir constant *(K_L)*through equation 12 facilitates the calculation of $\Delta G°$ for each

temperature, as depicted in Table 11. The van't Hoff equation (eq. 14), illustrated in Figure 5-d, allows for the estimation of $\Delta H°$ and $\Delta S°$ by plotting $ln\ K_c$ against $1/T$, with the slope and intercept yielding enthalpy and entropy values, respectively [43, 44].

$$K_C = 10^6 K_L \tag{12}$$

$$\Delta G° = -RT \ln K_C \tag{13}$$

$$\ln K_C = \left(\frac{-\Delta H°}{R}\right) \times \frac{1}{T} + \frac{\Delta S°}{R} \tag{14}$$

The thermodynamic parameters presented in Table 11 elucidate the nature of the adsorption process. A negative $\Delta G°$ value signifies the spontaneous nature of the adsorption, indicating it proceeds without external energy input. The sign and magnitude of $\Delta S°$ reveal the adsorption mechanism, with a positive $\Delta S°$ suggesting a dissociative process. The enthalpy change, $\Delta H°$, reflects the heat exchanged at constant pressure, with a positive value indicating an endothermic reaction. The observation that adsorption capacity increases with temperature corroborates the endothermic nature of the process [43, 45]. Furthermore, the relatively low value of the enthalpy indicate there is a physical adsorption and its positive sign means the amount of energy needed for that adsorption is more than that of released.

Table 11. Thermodynamic parameters of adsorption.

T (°C)	ΔG° (KJ/mol)	ΔH° (KJ/mol)	ΔS° (J/mol)
30	-30.019	5.337	81.502
45	-31.298		
60	-32.461		

4. Conclusion

The management of dyehouse textile effluents can pose a serious environmental challenge, drawing considerable attention from the research community. This issue is further compounded in the context of natural dyes, where a substantial fraction remains unadsorbed, persisting in wastewater. In this study, we explored the efficacy of a MOF, specifically MIL-53 (Al), in the adsorptional removal of cochineal dye, one of the most prevalent natural red dyes in the textile industry. This research studied the dye removal efficiency, examining the influence of several factors including adsorbent quantity, pH, temperature, and contact time, utilizing the RSM for optimization. The findings indicated that the adsorbent amount markedly impacted dye removal, while temperature exerted the least influence. An optimization equation was developed, demonstrating minimal discrepancy with experimental outcomes, highlighting its reliability. Kinetic analyses revealed that the adsorption process predominantly follows the pseudo-second-order model. The calculated activation energy (4.914 KJ/mol) underscores a predominantly physical adsorption mechanism onto the porous structure of MIL-53 (Al). Isotherm studies further affirmed the Langmuir model as the most suitable descriptor of the adsorption process, noting an increase in adsorption capacity with temperature elevation. At the top temperature examined (60°C), the adsorption capacity reached 178.57 mg/g. Thermodynamic investigations corroborated these findings, revealing a positive enthalpy change (5.337 KJ/mol) indicative of an endothermic process, aligning with the physical adsorption mechanism suggested by kinetic studies. The favorable adsorption of the dye by this adsorbent is due to its porosity, high surface area and the presence of the benzene structure in the ligand, which makes π-π stacking possible. This comprehensive approach

not only underscores the potential of MIL-53 (Al) in treating dye-laden effluents but also offers insight into optimizing conditions for enhanced dye removal, contributing valuable knowledge to the field of wastewater treatment in the textile industry. Future studies can focus on the effects of MIL-53 (Al) structure, and preparation parameters on the adsorption behaviour of natural dyes.

Acknowledgement

This work has been supported by the Center for International Scientific Studies & Collaborations (CISSC). Ministry of Science Research and Technology.

5. References

[1] Holkar CR, Jadhav AJ, Pinjari DV, Mahamuni NM, Pandit AB. A critical review on textile wastewater treatments: possible approaches. Journal of environmental management. 2016; 182:351-66. https://doi.org/10.1016/j.jenvman.2016.07.090

[2] Yaseen DA, Scholz M. Textile dye wastewater characteristics and constituents of synthetic effluents: a critical review. International journal of environmental science and technology. 2019; 16:1193-226. https://doi.org/10.1007/s13762-018-2130-z

[3] Kant R. Textile dyeing industry an environmental hazard. 2012. https://www.doi.org/10.4236/ns.2012.41004

[4] Pizzicato B, Pacifico S, Cayuela D, Mijas G, Riba-Moliner M. Advancements in sustainable natural dyes for textile applications: A review. Molecules. 2023; 28(16):5954. https://doi.org/10.3390/molecules28165954

[5] Imani H, Gharanjig K, Ahmadi Z. A novel efficient method for eco-friendly deep dyeing of wool yarns by extracted madder dyes in the presence of additives. Indust Crops Products. 2022; 183:114970. https://doi.org/10.1016/j.indcrop.2022.114970

[6] Ammayappan L, Jose S. Functional Aspects, Ecotesting, and Environmental Impact of Natural Dyes. In: 1st ed. Taylor & Francis Group; 2015.

[7] Hosseinnezhad M, Gharanjig K, Rouhani S, Razani N, Imani H. Environmentally friendly dyeing of wool yarns using of combination of bio-mordants and natural dyes. Environ Prog Sustain Energy. 2022;n41(5):e13868. https://doi.org/10.1002/ep.13868

[8] Mahmoodi NM, Arami M, Gharanjig K. Laboratory studies and CFD modeling of photocatalytic degradation of colored textile wastewater by titania nanoparticles. Desalination Water Treatment. 2009; 1(1-3):312-7. https://doi.org/10.5004/dwt.2009.128

[9] Khorramfar S, Mahmoodi NM, Arami M, Gharanjig K. Equilibrium and kinetic studies of the cationic dye removal capability of a novel biosorbent Tamarindus indica from textile wastewater. Color Technol. 2010; 126(5):261-8. https://doi.org/10.1111/j.1478-4408.2010.00256.x

[10] Quispe-Quispe A, Pérez-Falcón LF, Quispe-Marcatoma J, Landauro CV, Peña Rodriguez VA. Removal of Cochineal Dye Color through Atmospheric Pressure Plasma Discharge Jet. Appl Sci. 2024; 14(2):680. https://doi.org/10.3390/app14020680

[11] Ammayappan L, Shakyawar DB. Dyeing of carpet woolen yarn using natural dye

from cochineal. J Nat Fibers. 2016; 13(1):42-53. https://doi.org/10.1080/15440478.2014.984054

[12] Shams Nateri A, Dehnavi E, Hajipour A, Ekrami E. Dyeing of polyamide fibre with cochineal natural dye. Pigm Resin Technol. 2016; 45(4):252-8. https://doi.org/10.1108/PRT-05-2015-0043

[13] Imani H, Gharanjig K, Ahmadi Z. Eco-friendly single bath dyeing of wool yarns with extracted cochineal dye: optimization and additives effect. Pigm Resin Technol. 2023; 52(3):321-30. https://doi.org/10.1108/PRT-04-2022-0048

[14] Bhatia D, Sharma NR, Singh J, Kanwar RS. Biological methods for textile dye removal from wastewater: A review. Critical Rev Environ Sci Technol. 2017; 47(19):1836-76. https://doi.org/10.1080/10643389.2017.1393263

[15] Su CX, Low LW, Teng TT, Wong YS. Combination and hybridisation of treatments in dye wastewater treatment: a review. J Environm Chem Eng. 2016; 4(3):3618-31. https://doi.org/10.1016/j.jece.2016.07.026

[16] Piaskowski K, Świderska-Dąbrowska R, Zarzycki PK. Dye removal from water and wastewater using various physical, chemical, and biological processes. J AOAC Inter. 2018; 101(5):1371-84. https://doi.org/10.5740/jaoacint.18-0051

[17] Rashid R, Shafiq I, Akhter P, Iqbal MJ, Hussain M. A state-of-the-art review on wastewater treatment techniques: the effectiveness of adsorption method. Environ Sci Poll Res. 2021; 28:9050-66. https://doi.org/10.1007/s11356-021-12395-x

[18] Bal G, Thakur A. Distinct approaches of removal of dyes from wastewater: A review. Mater Today: Proc. 2022; 50:1575-9. https://doi.org/10.1016/j.matpr.2021.09.119

[19] Uddin MJ, Ampiaw RE, Lee W. Adsorptive removal of dyes from wastewater using a metal-organic framework: A review. Chemosphere. 2021; 284:131314. https://doi.org/10.1016/j.chemosphere.2021.131314

[20] Naghdi S, Shahrestani MM, Zendehbad M, Djahaniani H, Kazemian H, Eder D. Recent advances in application of metal-organic frameworks (MOFs) as adsorbent and catalyst in removal of persistent organic pollutants (POPs). J Hazard Mater. 2023; 442:130127. https://doi.org/10.1016/j.jhazmat.2022.130127

[21] Ma X, Tan J, Li Z, Huang D, Xue S, Xu Y, Tao H. Fabrication of stable MIL-53 (Al) for excellent removal of rhodamine B. Langmuir. 2022; 38(3):1158-69. https://doi.org/10.1021/acs.langmuir.1c02836

[22] Nguyen LM, Nguyen NT, Nguyen TT, Nguyen DH, Nguyen DT, Van Tran T. Facile synthesis of $CoFe_2O_4$@ MIL-53 (Al) nanocomposite for fast dye removal: Adsorption models, optimization and recyclability. Environ Res. 2022; 215:114269. https://doi.org/10.1016/j.envres.2022.114269

[23] Allahbakhshi M, Mahmoodi NM, Mosaferi M, Kazemian H, Aslani H. Synthesis of functionalized metal-organic framework metal-organic framework (MIL-53)/Chitosan for removing dye and pharmaceuticals. Surf Inter. 2022; 35:102471. https://doi.org/10.1016/j.surfin.2022.102471

[24] Allahbakhshi M, Mahmoodi NM, Mosaferi M, Kazemian H. Amine-functionalized metal-organic framework/graphene oxide nanocomposite for the removal of Direct Red 23 from water. Inorg Chem Commun. 2023; 154:110943. https://doi.org/10.1016/j.inoche.2023.110943

[25] Mehrparvar L, Safapour S, Sadeghi-Kiakhani M, Gharanjig K. Chitosan-

polypropylene imine dendrimer hybrid: a new ecological biomordant for cochineal dyeing of wool. Environ Chem Lett. 2016; 14:533-9. https://doi.org/10.1007/s10311-016-0559-1

[26] Imanipoor J, Mohammadi M, Dinari M, Ehsani MR. Adsorption and desorption of amoxicillin antibiotic from water matrices using an effective and recyclable MIL-53 (Al) metal–organic framework adsorbent. J Chem Eng Data. 2020; 66(1):389-403. https://doi.org/10.1021/acs.jced.0c00736

[27] Karimifard S, Moghaddam MR. Application of response surface methodology in physicochemical removal of dyes from wastewater: a critical review. Sci Total Environ. 2018; 640:772-97. https://doi.org/10.1016/j.scitotenv.2018.05.355

[28] Sadeghi-Kiakhani M, Arami M, Gharanjig K. Application of a biopolymer chitosan-poly (propylene) imine dendrimer hybrid as an antimicrobial agent on the wool fabrics. Iranian Poly J. 2013; 22:931-40. https://doi.org/10.1007/s13726-013-0193-8

[29] Noble D. FT-IR spectroscopy. Anal Chem. 1995; 67(11):381A-5A.

[30] Revellame ED, Fortela DL, Sharp W, Hernandez R, Zappi ME. Adsorption kinetic modeling using pseudo-first order and pseudo-second order rate laws: A review. Clean Eng Technol. 2020; 1:100032. https://doi.org/10.1016/j.clet.2020.100032

[31] Benjelloun M, Miyah Y, Evrendilek GA, Zerrouq F, Lairini S. Recent advances in adsorption kinetic models: their application to dye types. Arabian J Chem. 2021; 14(4):103031. https://doi.org/10.1016/j.arabjc.2021.103031

[32] Wang J, Guo X. Adsorption kinetic models: Physical meanings, applications, and

solving methods. J Hazard Mater. 2020; 390:122156. https://doi.org/10.1016/j.jhazmat.2020.122156

[33] Hubbe MA, Azizian S, Douven S. Implications of apparent pseudo-second-order adsorption kinetics onto cellulosic materials: A review. BioResources. 2019; 14(3).

[34] Singh VK, Kumar EA. Comparative studies on CO_2 adsorption kinetics by solid adsorbents. Energy Procedia. 2016; 90:316-25. https://doi.org/10.1016/j.egypro.2016.11.199

[35] Inglezakis VJ, Zorpas AA. Heat of adsorption, adsorption energy and activation energy in adsorption and ion exchange systems. Desalination Water Treat. 2012; 39(1-3):149-57. https://doi.org/10.1080/19443994.2012.669169

[36] Li C, Xiong Z, Zhang J, Wu C. The strengthening role of the amino group in metal–organic framework MIL-53 (Al) for methylene blue and malachite green dye adsorption. J Chem Eng Data. 2015; 60(11):3414-22. https://doi.org/10.1021/acs.jced.5b00692

[37] Gouamid MO, Ouahrani MR, Bensaci MB. Adsorption equilibrium, kinetics and thermodynamics of methylene blue from aqueous solutions using date palm leaves. Energy Procedia. 2013; 36:898-907. https://doi.org/10.1016/j.egypro.2013.07.103

[38] Abin-Bazaine A, Trujillo AC, Olmos-Marquez M. Adsorption isotherms: enlightenment of the phenomenon of adsorption. Wastewater Treatment. 2022; 19:1-5.

[39] Kalash KR, Al-Furaiji MH, Waisi BI, Ali RA. Evaluation of adsorption

performance of phenol using non-calcined Mobil composition of matter no. 41 particles. Desalin Water Treat. 2020; 198:232-40. https://www.doi.org/10.5004/dwt.2020.26018

[40] Sağlam S, Türk FN, Arslanoğlu H. Use and applications of metal-organic frameworks (MOF) in dye adsorption. J Environ Chem Eng. 2023; 20:110568. https://doi.org/10.1016/j.jece.2023.110568

[41] Al Sharabati M, Sabouni R. Selective removal of dual dyes from aqueous solutions using a metal organic framework (MIL-53 (Al)). Polyhedron. 2020; 190:114762. https://doi.org/10.1016/j.poly.2020.114762

[42] Yılmaz E, Sert E, Atalay FS. Synthesis, characterization of a metal organic framework: MIL-53 (Fe) and adsorption mechanisms of methyl red onto MIL-53 (Fe). J Taiwan Institute Chem Eng. 2016; 65:323-30. https://doi.org/10.1016/j.jtice.2016.05.028

[43] Ebelegi AN, Ayawei N, Wankasi D. Interpretation of adsorption thermodynamics and kinetics. Open J Phys Chem. 2020; 10(03):166-82. https://doi.org/10.4236/ojpc.2020.103010

[44] Tran HN, You SJ, Chao HP. Thermodynamic parameters of cadmium adsorption onto orange peel calculated from various methods: A comparison study. J Environ Chem Eng. 2016; 4(3):2671-82. https://doi.org/10.1016/j.jece.2016.05.009

[45] Saha P, Chowdhury S. Insight into adsorption thermodynamics. Thermodynamics. 2011 Jan 14;16:349-64.